New Insights about the Importance of the Alteration Layer/Glass Interface

Magaly Tribet[1]*, Anamul H. Mir[2], Célia Gillet[1], Christophe Jégou[1], Sarah Mougnaud[1], Jonathan. A. Hinks[2], Stephen. E. Donnelly[2], Sylvain Peuget[1]

[1]CEA, DES, ISEC, DE2D/SEVT, University of Montpellier, Marcoule, France

[2]MIAMI Irradiation Facility, School of Computing and Engineering, University of Huddersfield, UK

*corresponding author (magaly.tribet@cea.fr)

1 Abstract

This work addresses the impact of radiation damage on the leaching of international simple glass (ISG). Pristine and specimens irradiated with multi-energy Au ions were leached for 82 days at 90 °C in pure water and pH 9 and regularly sampled. Samples leached for 13 and 58 days were characterized using transmission electron microscopy (TEM) to study the microstructure(s) of the alteration layers formed from the radiation-damaged and pristine glasses. Furthermore, a sample altered for 82 days was immersed in water enriched in isotopically tagged water molecules ($H_2{}^{18}O$) to study and compare the mobility and reactivity of water at room temperature in the alteration layers formed on these glasses. The studies revealed that radiation damage diminished the chemical durability of the ISG glass since the beginning of the leaching experiment. Concomitantly, the formation of a non-porous alteration layer of about 237 nm after 13 days of leaching evolving into the formation of a nanoporous alteration layer of about 570 nm after 58 days of leaching was observed in the irradiated glasses. In contrast, a non-porous altered layer of about 138 nm only developed in the non-irradiated specimen altered for 58 days. Using energy-filtered transmission electron microscopy, the altered layers in all the cases were found to be depleted in boron, in agreement with the time of flight secondary ion mass spectroscopy studies. Despite pore formation, similar behaviour in the ^{18}O — ^{16}O exchanges (with respect to the uncertainties) was observed in the major part of the alteration layers whether formed from the irradiated or pristine ISG, leading to the conclusion that the greater alterability of the radiation-damaged ISG may not be due to the porosity. However, isotopic exchanges also revealed a significantly higher reactivity of water in the alteration-layer/glass interface for the irradiated glass. While these studies provide important insights about the role of porosity and radiation damages, they also highlight the complex nature of glass dissolution and suggest that studies directed at alteration-layer/glass interface are needed to better understand and explain the mechanisms controlling the glass dissolution in the residual alteration rate regime.

2 Introduction

Glasses due to their ease of manufacture and flexibility to accommodate a variety of elements in their structure are used as nuclear waste conditioning matrices around the world. To address the release and transport of radionuclides from such wasteforms, it is important to understand the mechanisms of glass leaching and the way in which various factors such as pH, temperature, glass composition and self-irradiation damage play a role in it. Although the fundamental leaching mechanisms of glasses, such as water penetration and interdiffusion [1-4], hydrolysis of the bonds [5,6], condensation [6-8] and, precipitation of secondary phases in certain cases [8,9] are well described, the specific mechanisms controlling glass dissolution in the long-term and the role played by radiation damage are still debated in the literature. A universally accepted picture of glass dissolution incorporating the impact of radiation damage is yet to emerge. In recent years, two fundamentally different limiting mechanisms of glass leaching in the long-term alteration regime have been the focus of researchers [6,7,10-15]. The interface-coupled dissolution-precipitation (ICDP) [6,11,12,16] model proposes simultaneous hydrolysis and

precipitation at the glass-water interface leading to inward progress of the leaching front and formation of the so-called surface alteration layer (SAL). The SAL, as depicted in Figure 1, is also referred to as the alteration-layer/glass interface or reactive interface in the literature. Transport of glass constituents and water through the precipitated SAL eventually controls the rate of leaching explaining the rate drop and approach to the so-called "residual rate" of glass alteration/leaching. The second model, on the other hand, proposes inter-diffusion and ion exchange as the fundamental mechanisms for glass leaching and the formation of the alteration layer, followed by progressive in-situ hydrolysis/re-condensation [7,10,13-15]. In this model, mobile elements are ion-exchanged (Na, Ca) or hydrolysed (B) with water (H^+/H_3O^+) resulting in the formation of silanol groups (Si-OH) in the ion-exchanged region which eventually transforms into the alteration layer via condensation reactions ($2SiOH \rightleftharpoons Si\text{-}O\text{-}Si + H_2O$). In this case, the alteration layer region called gel (Figure 1) as a diffusive barrier is the transport limiting factor explaining the residual alteration rate regime. Nevertheless, none of these models directly address or take into account the effect of ion irradiation on the microstructure of the alteration layer, including the SAL part, at nano-scale. It is essentially the aspect of radiation damage that will be the focus of this study.

A majority of the studies on the long-term leaching behaviour have mainly focused on the impact of beta and gamma radiation [17-20]. The predominant role of alpha decay of minor actinides on the long-term radiation component has only been recently highlighted [17]. Indeed, the alpha irradiation ageing of the glass will cause significant changes in its structure and properties [17,21,22]. Due to the various complexities associated with handing and characterizing radioactive specimens, ion irradiation has been widely used as a proxy to simulate the effects of self-irradiation damage. It was recently observed in the literature that the alteration behaviour of borosilicate glasses was significantly modified by the prior external irradiation by heavy ions [22-24], specifically, during the residual alteration rate regime [22,23]. Radiation damage was observed to result in an alteration layer around 4 times thicker than the one formed on a non-irradiated glass leached under the same conditions. The evolution of the leaching rate with irradiation dose was attributed to the effects of nuclear collisions [23], essentially, following the trend as observed in the structural and mechanical properties with nuclear dose. Also, the altered thickness evolved as a square root of time, indicating that the actual alteration rate versus time diminished on both the irradiated and non-irradiated samples [23]. These observations suggest that the effects of irradiation on the alteration mechanisms (in the residual rate regime) are linked to the changes in either the glass structure and/or its properties. These modifications potentially induce an increase in water migration and/or an increase in the reactivity in the alteration layer formed from the irradiated glass (making it less passivating than the one formed from a non-irradiated glass).

In the present communication, we aim to better understand which part of the alteration layer formed from an irradiated glass is modified in terms of its passivating properties that could explain the increased residual rate and the formation of a thicker alteration layer. As the microstructure of altered glasses is still poorly understood and there are currently no studies focusing on the microstructure of the radiation-damaged and leached ISG, this article aims to use transmission electron microscopy (TEM) and energy-filtered TEM (EFTEM) at cryogenic temperatures to study and compare the microstructure of the non-irradiated and irradiated ISG glass after various leaching intervals. The leaching tests were conducted under the same conditions as reported earlier [23]. Furthermore, as the gel reorganization and its formation from the glass (at the gel/glass interface) involves dissociation of oxygen bonds, a specific experiment was performed by using isotopically tagged water molecules ($H_2{}^{18}O$) to assess the water ingress and oxygen exchanges through the alteration layers formed from the irradiated and non-irradiated glasses. By following ^{18}O — ^{16}O exchanges versus time and depth, it was possible to access the self-organization ability of the alteration layers obtained from irradiated or non-irradiated glasses at ambient temperature [7] and the role of porosity.

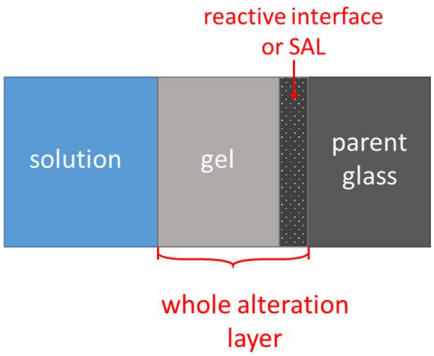

Figure 1: A schematic view of the alteration and associated terminology used in the present publication.

3 Experimental methodology

An overview of the experimental scheme is presented in Figure 2. Several ISG glass specimens (6.25×12.5×1 mm^3) were partially masked with a thick Al foil to maintain a non-irradiated reference area and then irradiated with multi-energy gold ions (0.5 to 3.5 MeV) for various fluences up to a maximum of 5.5×10^{14} $ions.cm^{-2}$ to attain a uniform and saturation damage state up to a depth of about 1000 nm (Figure 2(a)). Details of this ion irradiation are presented elsewhere [23]. After ion irradiation, the Al mask was removed and the specimens were leached for up to 82 days at 90 °C in water under static conditions (Figure 2(b)). The experiment involved placing the irradiated glass monoliths in a PFA-Teflon reactor, covering them by an ISG glass powder bed (40-63 µm mean size) and adding deionized water. The mass of the glass powder was adjusted to yield a glass-surface-area to solution-volume ratio (S/V) of 200 cm^{-1} in order to quickly attain saturation with respect to Si (within one day) so as to focus on the residual rate regime of the leaching. A pH of 9 (± 0.1) at 90°C was measured from the first day to the end of the leaching experiment. The leached specimens were sampled regularly (13, 32, 40, 58 and 82 days) and mainly analysed using ToF-SIMS. The ToF-SIMS results have been published in an earlier article [23]. A dependence of alteration layer thickness on the irradiation dose was observed in the earlier work for fluences less than 3.7×10^{13} $ions.cm^{-2}$ whereas for larger fluences a saturation in the alteration thickness was attained (figure 5 in S. Mougnaud *et al.* [23]). Figure 6 from the previous article is reproduced here in Figure 2(f) showing the alteration thickness as a function of the leaching time for the irradiated (dose at saturation) and non-irradiated specimens.

3.1 TEM specimen preparation and characterizations

Specimens altered for 13 and 58 days, as indicated by the rectangles in Figure 2(f), were selected for microstructural characterisation using TEM in the current study. These particular specimens were chosen to probe the microstructure of the leached specimens in the first days of alteration — when the alteration layer forms and the differences because of the previous irradiation were already clearly observable — and when the residual leaching rate is well established (58 days) (this can be seen from the ToF-SIMS data presented in Figure 2(f)).

Before making the specimens for the TEM analysis, the leached specimens were coated with 100 - 200 nm of Cr (Figure 2(c)) using a Quorum QT150T sputter coater to avoid any charging and surface damage during specimen preparation using the focussed ion beam system (FIB). A region of interest on the irradiated and non-irradiated areas of the corroded specimens was then deposited with carbon (2 µm thick) to prevent any ion beam damage during specimen preparation (Figure 2(c)). The specimens for TEM analysis were then prepared using 30 keV Ga ions and standard FIB procedures. Using a Hitachi 9500 TEM and a Gatan liquid-nitrogen cooled TEM specimen holder, the specimens were cooled to –130 °C for TEM/EFTEM analysis (Figure 2(d)). The low temperature was chosen to reduce the extent of

electron beam damage. The distribution of pores in the TEM images of the corroded specimens was analysed using Fiji software [25]. The images were first thresholded to define the background level and then using the particle analysis tool of Fiji, the pores were fitted with circles to evaluate pore diameters.

3.2 Immersion in $H_2{}^{18}O$ at ambient temperature

A specimen altered for 82 days, as described previously, was considered here. This specimen had been irradiated up to a total fluence of 4.6 x 10^{14} ions.cm^{-2} (note that as described in S. Mougnaud et al.[23], the damage saturation occurred after about 3.7 x 10^{13} ions.cm^{-2}). The alteration layer thicknesses were measured by ToF-SIMS both on the irradiated zone (IZ) and the non-irradiated zone (NIZ) to be respectively of 586 and 162 nm (± 10%). This altered specimen was then immersed at 25 ± 2 °C in a solution of $H_2{}^{18}O$ with $^{18}O/^{16}O$ = 1.45 ± 0.06 for 143 days (i.e. 3413 hours) and sampled regularly in order to record the oxygen isotopic profiles in the alteration layer by ToF-SIMS as described in [7] and as illustrated in Figure 2~~Figure 2~~(e). It has been previously shown that in these conditions, the analytical protocol of $^{18}O/^{16}O$ is accurate [7] and that the glass sample did not leach significantly.

The ToF-SIMS analyses were performed by Tescan Analytics, Fuveau, France, using a ToF-SIMS 5 spectrometer (IonTof—Munster, Germany). The analytical procedure was optimized to minimize the exchange between pore water and air humidity and, to quantify the oxygen isotopic ratio in the alteration layer. For ToF-SIMS, a pulsed 25 keV ~0.03-pA Bi_3^{++} primary ion source was employed over a rastered area of 50 µm × 50 µm (beam size ≤ 3 µm). Depth profiling (negative ion mode) was performed using a 1-keV Cs^+ sputter beam with a 90-nA target current over a 200-µm x 200-µm area. An electron flood gun was used to avoid the specimen charging. A 1D profilometer was used to measure the final crater depth at the end of the analysis. Data was then displayed as a function of depth considering the same sputtering rate in the alteration layer and in the pristine glass. The natural $^{18}O/^{16}O$ ratio in the glass before immersion was established by first analysing a non-altered ISG glass coupon, containing both an irradiated zone and a non-irradiated zone. Finally, the $^{18}O/^{16}O$ profiles were normalized to reach the natural abundance (2.05×10^{-3}) in the non-altered glass [7].

The results are then presented in terms of δ versus time, according to equation 1 [26], where $^{18}O/^{16}O$ is the atomic ratio of ^{18}O to ^{16}O and the reference, $(\frac{^{18}O}{^{16}O})_{glass}$, refers to the ($^{18}O/^{16}O$) ratio measured by ToF-SIMS in the non-altered glass part, and very close to the natural abundance.

$$\delta = \frac{\left(\frac{^{18}O}{^{16}O}\right) - (\frac{^{18}O}{^{16}O})_{glass}}{(\frac{^{18}O}{^{16}O})_{glass}} \qquad \text{Equation 1}$$

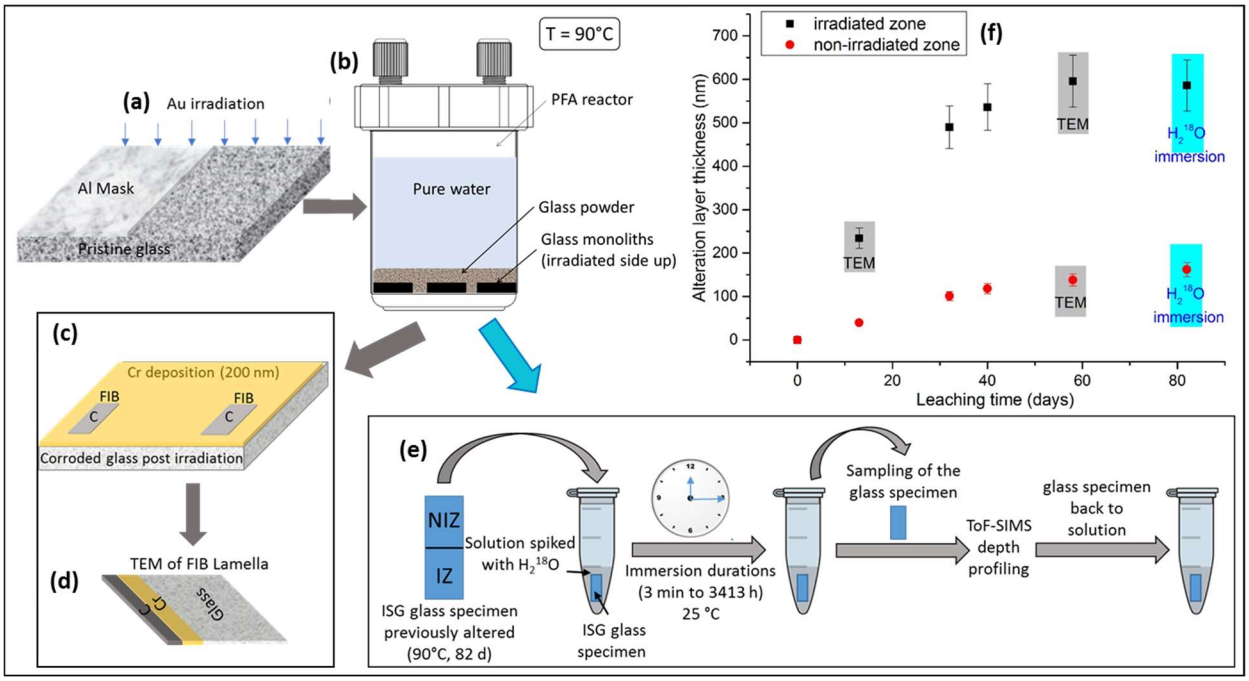

Figure 2 : An overview of the experimental methodology. (a) Partially masked ISG specimens were first irradiated with 0.5 to 3.5 MeV Au ions; (b) The mask was removed and the irradiated specimens were altered for up to 82 days at pH 9 and 90 °C; (c) The specimens were taken out and protective layers of Cr and C were deposited on the leached specimens to prepare the FIB TEM lamellae; (d) The thin FIB TEM lamellae were characterized using the TEM; (e) Implementation of the sequences of a glass specimen immersion in $H_2{}^{18}O$ and analyses by ToF-SIMS (IZ and NIZ stand for irradiated and non-irradiated zone respectively) ; (f) ToF-SIMS results from an earlier study showing the alteration thickness as a function of the leaching time for the pristine and irradiated specimens, at saturation dose [23]. The grey and blue rectangles indicate the specimens analysed by TEM in the current study (13 days and 58 days of leaching) and the specimen immersed in $H_2{}^{18}O$ (82 days of leaching), respectively.

4 Results

4.1 TEM characterization

4.1.1 The Microstructure of the non-irradiated altered region (58 days of leaching)

Bright-field TEM (BF-TEM) and EFTEM images of the lamella taken from the non-irradiated region of the specimen corroded for 58 days are shown in Figure 3. Figure 3(a) gives a low-magnification view of the lamella. Based on the transmitted intensity (mass thickness contrast), following regions (from right to left) can be identified: (i) Vacuum region, (ii) protective carbon coating deposited in the FIB system, (iii) protective chromium deposited using plasma sputter coater, (iv) a non-porous altered layer (NPL) of about 138 nm which is relatively brighter and, (v) the non-altered glass (NAG) which is relatively darker compared to the NPL. The transmitted intensity profile in the NPL and NAG is superimposed on the figure for visual aid. The EFTEM images showing boron, Cr and C are shown in the inset (a-1). The NPL was found to be depleted in boron as indicated by a dark band between the NAG and Cr layer in the inset. A higher magnification image of the glass (NAG+NPL) is shown in Figure 3(b) where the two regions can be clearly differentiated on the basis of the transmitted intensity (brightness). A higher magnification EFTEM image for boron distribution and boron intensity profile is shown in Figure 3(c). Figure 3(d) shows a higher magnification BF-TEM image to better visualize the microstructure of the NAG and NPL. Other than the contrast differences, no visible microstructural differences can be identified in the two regions. It is worth mentioning that the width of the NPL calculated both from the BF-TEM and EF-TEM images (~138 nm) is in excellent agreement with the ToF-SIMS analysis in our earlier study [23] and shown in Figure 2(f).

It is worth mentioning that because the microstructure of the non-irradiated specimen leached for 58 days did not show any major changes, except the loss of mobile elements, there was no reason to do the microstructural characterisation of the non-irradiated specimen leached for 13 days.

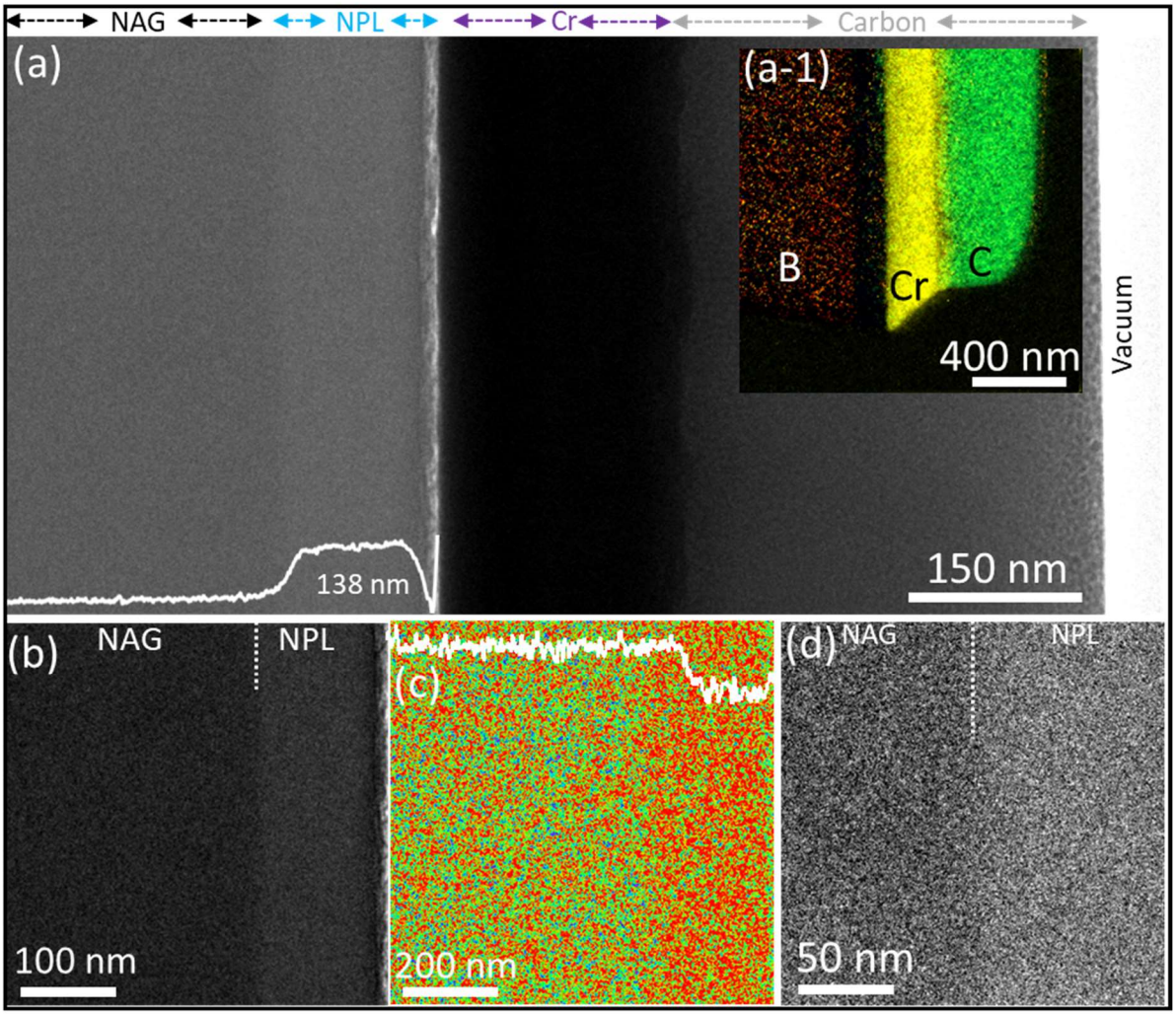

Figure 3: BFTEM and EFTEM images of the non-irradiated ISG glass corroded for 58 days at 90 °C and pH 9. (a) A low magnification BF-TEM image showing non-altered glass (NAG), a 138 nm wide non-porous altered layer (NPL), protective chromium, protective carbon and vacuum on the extreme right. A transmitted intensity line profile is superimposed on the glass to help differentiate the NAG and NPL. The inset (a-1) is an EFTEM image showing the distribution of B, Cr and C. The NPL appears as a darker band sandwiched between the NAG and Cr; (b) a higher magnification BF-TEM image only showing the NAG and NPL. The two are demarcated by a white dashed vertical line; (c) An EFTEM image showing the distribution of boron in the NAG and NPL. The superimposed line profile shows the boron intensity and, (d) a higher magnification BF-TEM image near the interface between the NAG and NPL to better visualize the microstructure at the nanoscale. Other than the brightness difference, no microstructural differences can be seen between the two regions.

4.1.2 The Microstructure of irradiated and altered regions (13 days and 58 days of leaching)

The BFTEM and EFTEM images of the lamella taken in the irradiated region of the specimen altered for 13 days are shown in Figure 4. It showed an alteration layer of about 237 nm in excellent agreement with the ToF-SIMS results (the superimposed line profile shows the transmitted electron intensity). The alteration layer was found to be depleted in boron as shown in the EFTEM images displayed in the inset-(a-1) and also in agreement with the published data[23]. No visible microstructural differences were found between the altered and the non-altered glass, nor between the alteration layers observed in this case and the non-irradiated glass altered for 58 days (except in the alteration thickness value).

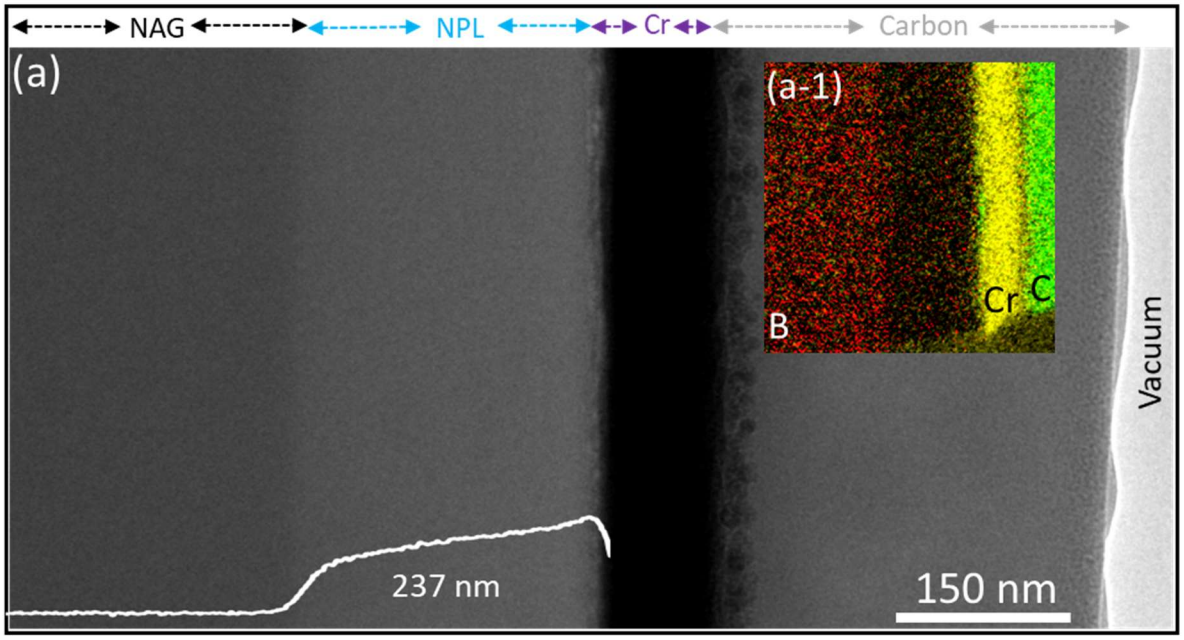

Figure 4: BFTEM and EFTEM images of the ISG glass irradiated with Au ions and then corroded for 13 days. The specimen showed a non-porous altered layer of 237 nm. The line profile shows the transmitted electron intensity and the inset (a-1) shows the EFTEM elemental maps. The altered layer was found to be depleted in boron.

The BFTEM and EFTEM images of the lamella taken in the irradiated region of the specimen altered for 58 days are shown in Figure 5. This specimen was also protected with Cr and C as in the previous case but, in this case, the protective layers started to come off during the TEM analysis. A low magnification image showing the partially detached Cr layer is shown in Figure S1 in the supplementary information (SI). Excluding the C and Cr layers, the following regions can be identified in the BF-TEM image (right to left): (i) Vacuum region, (ii) an alteration layer of lighter contrast (demarcated from the rest of the glass by a vertical dashed line) and, (iii) non-altered glass of slightly darker contrast. A higher magnification image of the alteration layer is shown in Figure 5(b). This layer can further be subdivided into at least two regions: (ii-a) an outer porous layer of about 490 nm referred as Microporous Layer (MiL) with an average pore size of about 1.5 ± 0.2 nm (see Figure 6(a) for the pore size distribution). A higher magnification image of the bright appearing pores is shown in Figure 5(d). (ii-b) A non-porous altered layer of about 80 ± 10 nm. The ± 10 nm error is due to the uncertainty in precisely locating the end of the MiL. A higher magnification image showing the MiL on the right-hand side and the NPL on the left-hand side for direct comparison is shown in Figure 5(c). A low magnification EFTEM image showing the boron distribution and the boron intensity profile in the altered and non-altered glass is shown in Figure 5(e). The width of the alteration layer was found to be about 570 nm (490 + 80 nm) which is in good agreement with the ToF-SIMS data (Figure 2(f)). A direct comparison of the irradiated and non-irradiated cases with leaching taking place from the top surface is presented in Figure 6(b). Besides clearly showing the variable thickness of the alteration layers, the presence of pores after 58 days in contrast to their lack after 13 days is noteworthy.

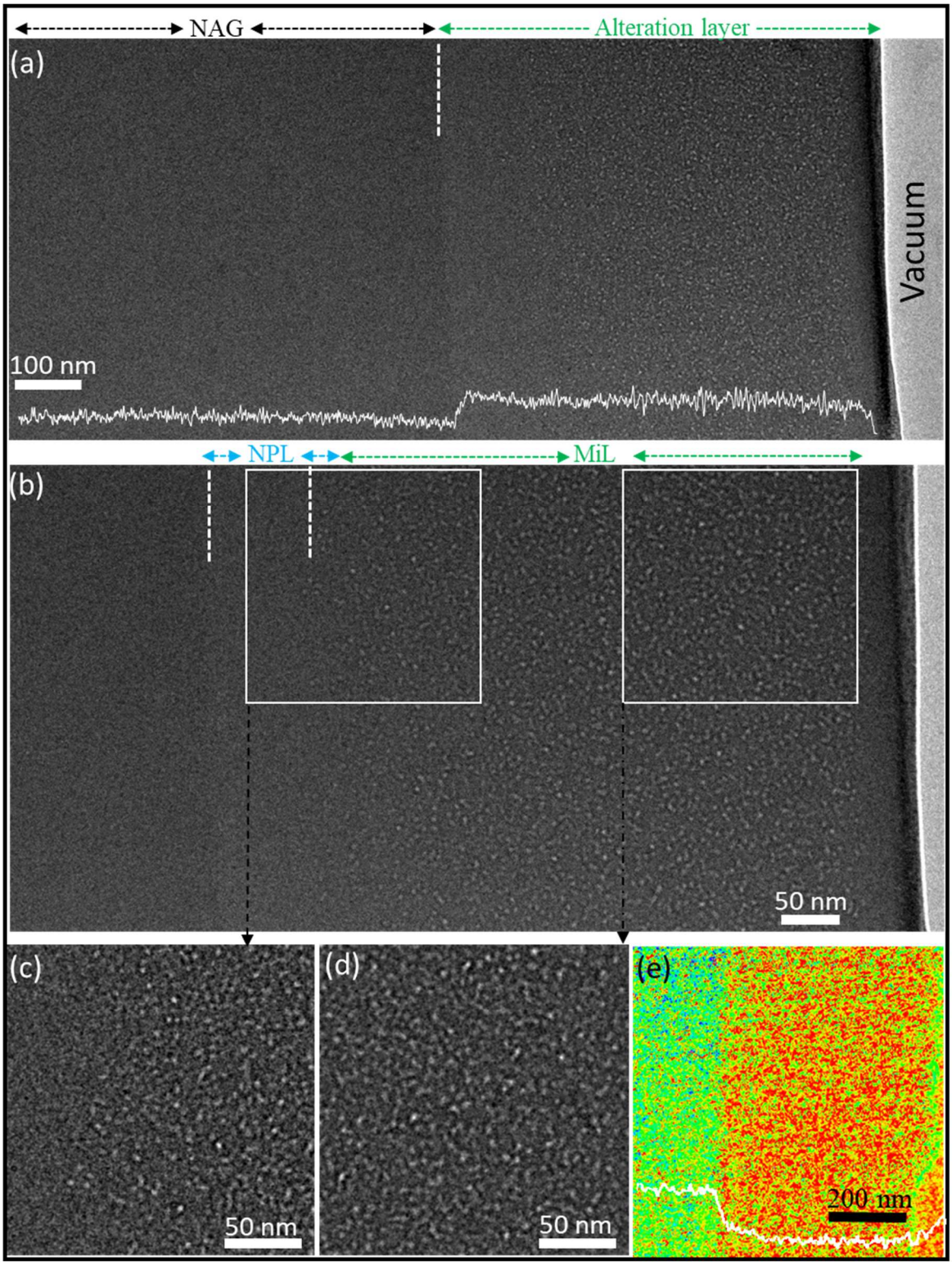

Figure 5: BF-TEM and EFTEM images of the ISG glass pre-irradiated with Au ions and then corroded for 58 days at 90 °C and pH 9. ***(a)*** *A low magnification BF-TEM image showing the non-altered glass (NAG) and an alteration layer of about 570 nm. A transmitted intensity profile is shown superimposed;* ***(b)*** *a higher magnification BF-TEM image to better visualize the porosity in the alteration layer. The alteration layer consisted of a microporous layer (MiL) of about 490 nm and a non-porous layer (NPL) of about 80 nm. The NPL region is roughly indicated by two vertical dashed lines;* ***(c)*** *a higher magnification image showing the NPL on the left-hand side and MiL on the right-hand side;* ***(d)*** *a higher magnification image showing the pores in the MiL; and,* ***(e)*** *an EFTEM image and boron intensity profile (in white) showing the distribution of boron in the non-altered glass and the alteration layer.*

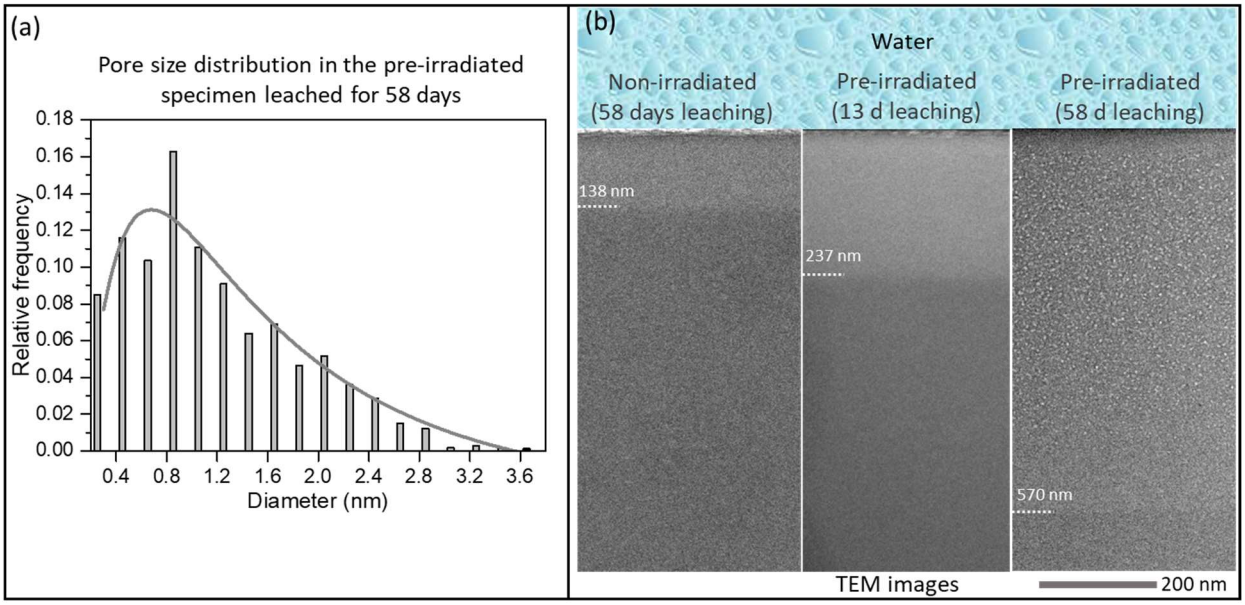

Figure 6: The distribution of porosity and a comparison of the effects of leaching. (a) The distribution of pores in the irradiated ISG specimen corroded for 58 days at 90 °C and pH 9. The solid line shows a log-normal fit; (b) a direct comparison of the effects of leaching on the Au irradiated and non-irradiated ISG glass corroded under the same conditions (90 °C, pH 9). The dashed lines and the numbers indicate the alteration layer boundary and its thickness. The non-irradiated glass leached for 58 days has a non-porous alteration layer of about 138 nm whereas the irradiated glass leached for 58 days has a combination of porous and non-porous alteration layer of about 570 nm. The irradiated glass leached for 13 days has a non-porous alteration layer of about 237 nm. The alteration layers in all the cases were depleted in boron.

4.2 Immersion in $H_2{}^{18}O$

The $^{18}O/^{16}O$ ratio and boron concentration profiles in the irradiated and non-irradiated zones respectively are presented in Figure 7~~Figure 7~~ for various durations of immersion in $H_2{}^{18}O$. First, it is worthy to note that the boron profiles confirm that the glass did not significantly alter during the immersion in $H_2{}^{18}O$ at 25 °C because the alteration layer thicknesses of (620 ± 20) and (165 ± 10) nm in the irradiated and non-irradiated zones respectively are in good agreement with the previously determined values just after leaching (as summarized in Table 1~~Table 1~~ (at ± 10%) [23]). Secondly, it was observed that for all contact durations, ^{18}O exchanged with ^{16}O in the whole alteration layer thickness and penetrated up to the so-called SAL (also called "reactive interface" in some studies) for both the irradiated and non-irradiated specimens. The $^{18}O/^{16}O$ ratio is in fact well defined in the TOF-SIMS by sharp anti-correlated changes in the boron concentration at the same time, as highlighted in Figure 8. Moreover, as also previously observed by Gin et al. [7], the increase of ^{18}O in the alteration layer was measurable even at the shortest contact time (3 min).

It can also be noticed that the $^{18}O/^{16}O$ profiles were mostly flat in a great part of the altered layer depth (called as "flat front" hereafter), whereas a spike was observed at the SAL. The "flat front" regions were respectively of 100 nm for the non-irradiated zone and 500 nm for the irradiated zone. Figure 9 presents the evolution of the normalized $^{18}O/^{16}O$ ratio, called δ, with time in the "flat front" parts of the irradiated and non-irradiated zones respectively. The differences observed between the non-irradiated and irradiated zones were within the uncertainty limits (from 10 to 20 % for each data point), implying that the number of exchanges between ^{16}O from the gel and ^{18}O from the tracing solution was very close in both the cases. However, slight differences can be noticed for the very short immersion times (see Figure 9(b)).

In both the zones (Figure 7~~Figure 7~~ and Figure 9), the ^{18}O concentration increased with the contact time, but slowed down and seemed to stabilize after around 1065 hours, which could reflect a possible saturation with time in the ^{18}O – ^{16}O exchanges.

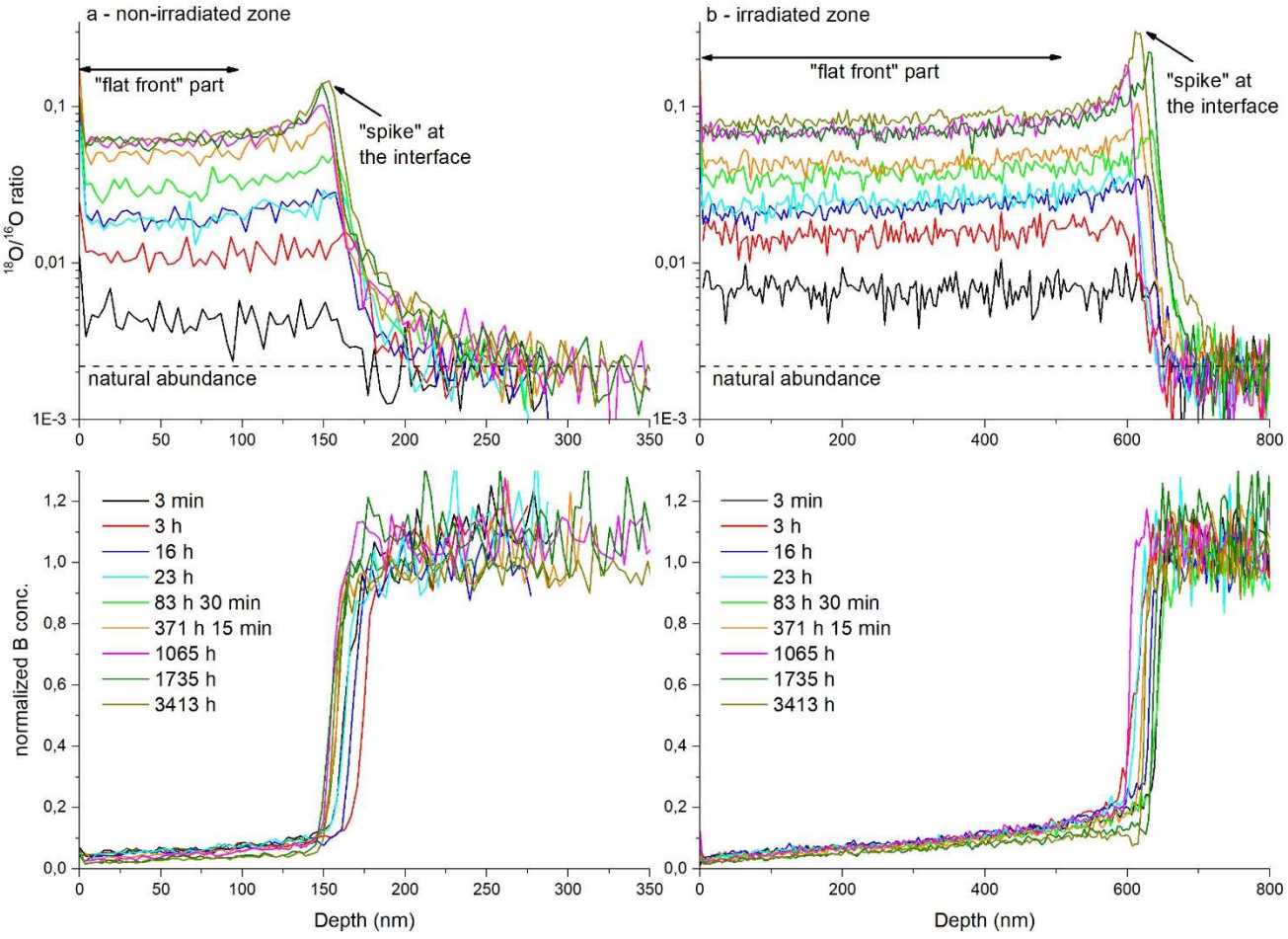

Figure 7: Evolution of the $^{18}O/^{16}O$ ratio versus depth (upper figures) and of the normalized boron concentration versus depth (lower figures). On the left (a), the profiles obtained from the non-irradiated zone are presented. On the right (b) the profiles obtained from the irradiated zone are presented. The dashed lines represent the natural $^{18}O/^{16}O$ abundance (2.05×10^{-3}).

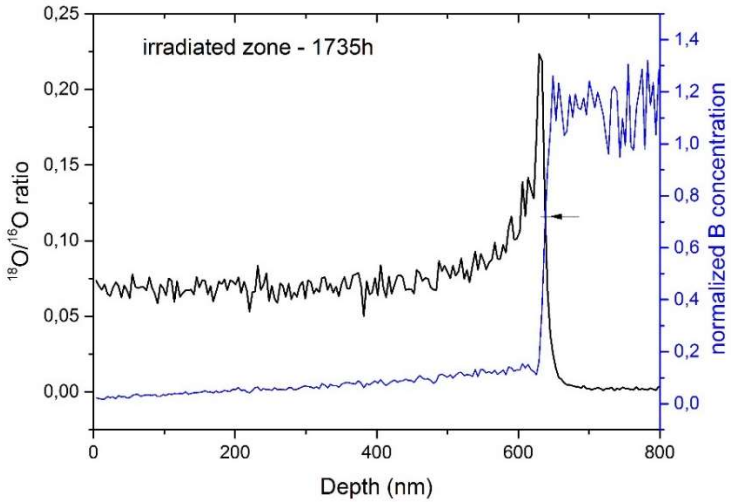

Figure 8: Comparison between the $^{18}O/^{16}O$ ratio profile and the boron concentration profile for the irradiated zone after 1735 hours of immersion in $H_2{}^{18}O$ enriched at 60%.

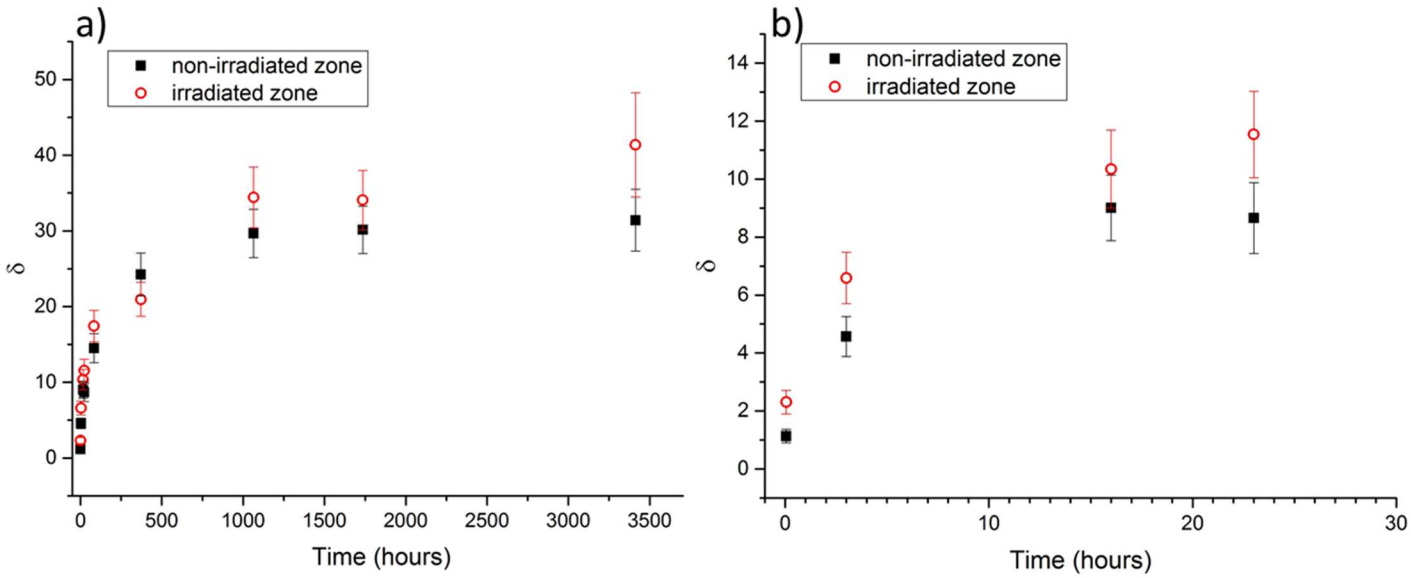

Figure 9: Evolution of δ, calculated in the "flat front" region of the alteration layers developed in the irradiated and non-irradiated zones, as a function of the contact time with $H_2{}^{18}O$ solution. Errors bars are calculated from the standard deviation on the values in the "flat front". a)-total immersion time and b) zoom of the first day of immersion (very short times).

However, an intense peak (called "spike") at the alteration-layer/glass interface (i.e. SAL) was observed (Figure 7~~Figure 7~~ and 8) for both the irradiated and non-irradiated zones, with a greater magnitude in the irradiated zone. This "spike" also increased with time in both the cases. In order to quantify the magnitude of the "spike" with time, its value was compared to the reference ratio in the glass, by using Equation 1 and the resulting δ is presented in Figure 10~~Figure 10~~, as a function of the immersion time, for the two zones (irradiated and non-irradiated). The data show a significant change in the value of δ versus time whether the parent glass was irradiated or not. For the longest contact time (3413 hours), the δ value was about 2.1 times higher at the interface in the irradiated zone compared to the interface in the non-irradiated zone and there was no obvious indication of its saturation even after 3413 hours. In conclusion, there was thus more isotopic exchange between the $H_2{}^{18}O$ and the altered layer in this "reactive interface" for the irradiated glass.

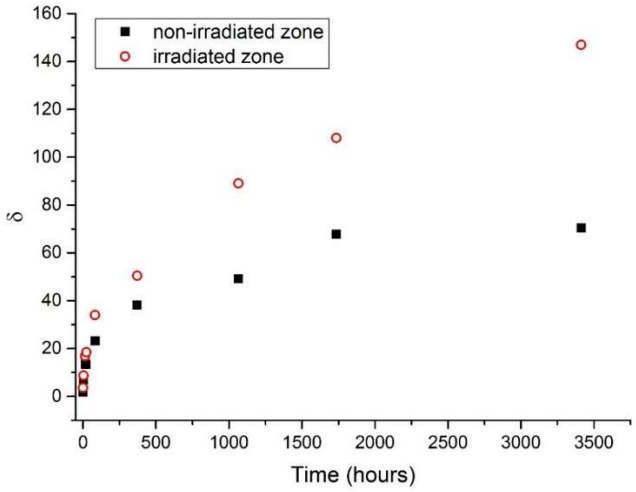

Figure 10 : Evolution of δ at the interface (spike signal at the interface) as a function of the immersion time for the two zones: the non-irradiated one (black) and the irradiated one (red).

4.3 Summary of the results

The results obtained in the present study, which aimed to finely characterize the alteration layer of the radiation-damaged and altered glasses, are summarized in Table 1~~Table 1~~. TEM showed no visible microstructural differences between the altered and the non-altered glass after 13 days, nor between the alteration layers observed on the irradiated glass altered for 13 days and the non-irradiated glass altered for 58 days (except in the thickness value). However, the microstructure and porosity of the irradiated glass evolved with leach time (13 days compared to 58 days), with the appearance of a microporous layer after 58 days with an average pore size of (1.5 ± 0.2) nm.

Isotopic exchanges of ^{18}O between $H_2{}^{18}O$ solution and ^{16}O from the alteration layer showed a similar behaviour (within 10 – 20 % of uncertainties) in the "flat front" region in the irradiated and non-irradiated zones. The ^{18}O isotope penetrated into the whole alteration thickness since the shortest contact time (3 min) and its ratio (compared to ^{16}O) increased with time, reaching saturation after 1065 hours. A "spike" in the ^{18}O — ^{16}O exchanges was observed at the interface between the alteration layer and the glass (i.e. SAL) with a greater magnitude (x 2.1 at the longest contact time) in the irradiated glass compared to the non-irradiated glass.

Alteration duration	**13 days**	**58 days**	**82 days**
Non-irradiated glass	(34 ± 4) nm [23]	(112 ± 12) nm [23] **TEM:** NPL of ~ 138 nm	(162 ± 17) nm [23] (165 ± 10) nm ($^{18}O/^{16}O$) **$^{18}O/^{16}O$ ratio:** "flat front" in the first 100 nm and spike at the SAL
Irradiated glass	(241 ± 25) nm [23] **TEM:** NPL of ~ 237 nm	(563 ± 57) nm [23] **TEM:** external micro-porous alteration layer (MiL~ 490 nm) and NPL of ~ 80 nm. Total ~ 570 nm In MiL : average pore size of (1.5 ± 0.2) nm	(586 ± 59) nm [23] (620 ± 20) nm ($^{18}O/^{16}O$) **$^{18}O/^{16}O$ ratio:** - "flat front" in the first 500 nm, with magnitude comparable to the non-irradiated area (± 10-20% uncertainties) - spike at the irradiated SAL, 2.1 times higher after 3413h than in the non-irradiated area.

Table 1 : Summary of the results obtained in the present study by TEM and $^{18}O/^{16}O$ exchanges. Comparison with data from [23].
NPL means "non-porous altered layer", MiL "micro-porous altered layer" and SAL "surface altered layer".

5 Discussion

An increase in the alterability of radiation-damaged ISG glasses has been previously observed using ToF-SIMS [23]. In the present study, the leached samples were characterized using TEM and subjected to tracing experiments with ^{18}O isotope. These experiments were aimed to: better understand the microstructure of alteration layers and its role in water transport; identify the leaching mechanisms; and, address how they are affected by radiation damage. From this perspective, the discussion is framed around the following questions:

(i) How does radiation damage affect the reactivity/leachability of the glass?
(ii) Why did the alteration layer in the irradiated ISG show porosity and not in the non-irradiated one?
(iii) Are the alteration layers, their reactivities and their passivation properties different in the irradiated and non-irradiated ISG?
(iv) Does porosity in the alteration layer play a role in water transport during leaching and does it affect the rate of leaching?
(v) Is it the entire alteration layer or the reactive interface (SAL) that controls the rate of leaching or alternatively, what is the rate-limiting step?

We will first focus on the potential impact of radiation damage to develop a fundamental picture of how radiation damage may affect various aspects of leaching and then eventually based on this understanding try to address rest of the questions.

5.1 Radiation damage and higher reactivity of the irradiated glasses

All irradiation studies whether on actinide doped specimens or on ion irradiated specimens have shown that radiation damage introduces several defects in the glass network. These defects are usually in the form of dangling bonds (non-bridging oxygen atoms and peroxy bridges), oxygen-deficient centres, molecular oxygen and coordination changes of certain network formers such as boron[21,22,27-30]. The mechanisms that dominate the leaching process should be affected because they eventually involve dissociation of bonds within the glass network — which itself is modified by the radiation damage. Therefore, radiation damage should directly play a role at this stage of leaching because it introduces dangling and strained bonds into the network thereby facilitating the process of leaching either by directly reducing the number of the bonds that need to be hydrolyzed or by facilitating the interaction of water with the strained bonds and other pre-existing defects. Radiation damage can also broaden the ring distribution [31,32] and thereby directly affect the diffusion barriers for water molecules [33]. More specifically for the case of the ISG glass and its simple and complex counterparts, the effects of ion irradiation have been extensively studied using both experimental approaches and atomistic simulations [21-23,27,29,31,34,35]. All these studies have shown that ion irradiation causes network depolymerization and transformation of 4-coordinated boron into 3-coordinated boron. For example, heavy-ion irradiations of the ISG glass have yielded a transformation of about 16 % of the 4-coordinated boron into 3-coordinated boron; depolymerization of the borosilicate network (formation of Q_3 units at the expense of Q_4 units); formation of molecular oxygen — either as a result of partial re-polymerization or/and due to a recombination of displaced oxygen atoms and, broadening of the ring distribution due to the formation of larger and smaller rings. Although detailed studies on how each of these modifications affects the leaching are still lacking, we will try to delve into this aspect in the following sections: the various irradiations induced modifications and their potential impact on the leaching are listed and addressed below.

5.1.1 Network depolymerization

Network depolymerization will lead to the formation of units such as Q_1, Q_2 and Q_3 at the expense of the Q_4 units. This can also generate defects such as non-bridging oxygen atoms which can react with water forming silanol groups. When comparing the irradiated and non-irradiated structures, it is therefore evident that a higher degree of hydrolysis is needed in the non-irradiated glass to break the bonds as compared to the irradiated glass where radiation damage acts as a source of the dangling bonds. Furthermore, MD simulations have shown that the energy barrier for the condensation of Q_n units increases as their connectivity increases. This is because increased connectivity requires a collective rearrangement upon condensation compared to the low connectivity Q_n units which only require local rearrangement [36]. Therefore, condensation reactions between Q_3 units are more difficult than between the Q_1 or Q_2 units. As radiation damage is known to increase the degree of network depolymerization, the irradiated glass should contain a higher proportion of depolymerized Q_n units and consequently undergo faster condensation for these highly depolymerized units. Thus, radiation damage can increase the rates of hydrolysis and condensation (i.e. higher chemical reactivity) consequently accelerating the process of leaching and subsequent structural relaxation of the leached glass. However, it can be noticed that the initial alteration rate of alpha-doped glasses and externally irradiated glasses[21,37,38], corresponding to the hydrolysis of the glassy network is not fundamentally modified compared to non-irradiated glasses. But these results correspond to the hydrolysis observed in very diluted medium. Is this information transposable to confined medium like what can happen in the SAL?

5.1.2 Transformation of BO_4 to BO_3

Kinetic Monte-Carlo simulations of leaching of sodium borosilicate and sodium alumino-borosilicate glasses indicate that irrespective of the glass composition an increase in the concentration of 3-coordinated boron leads to an increase in the rate of leaching [32]. These results are also supported by experimental studies of leaching of sodium borosilicate glasses as a function of boron content in the glass (from 0 to 75 mole % of B_2O_3)[39]. The experimentally measured normalized release rates of Na, Si and B adjusted for pH 9 as presented in Table 2 of ref [39] are plotted in Figure S2 in the SI as a function of the percentage of 3-coordinated boron atoms measured using NMR spectroscopy. The data show a consistent increase in the release rate of the elements with an increase in the fraction of the 3-coordinated boron species. In addition, NMR spectroscopy of altered ISG glass leached at pH 7 for 100 days at 90 °C has shown that the altered glass was slightly enriched in B (IV) compared to the non-altered one. This can be understood as a preferential release of B (III) during alteration [40]. In any case, one of the consequences of the irradiation-induced transformation of BO_4 to BO_3 is to free up the Na atoms. The freed Na atoms, in turn, lead to the formation of non-bridging oxygen atoms on silica tetrahedra making them vulnerable to attack by water (formation of silanol). Therefore, irradiation-induced transformation of 4-coordinated boron into 3-coordinated boron (about 16 % increase in the case of the ISG glass) and network depolymerization as a result of this transformation can both be expected to increase the rate of leaching due to higher leachability of the 3-coordinated boron atoms and higher chemical reactivity of the depolymerized network.

5.1.3 Formation of point defects

Energy barriers for various reactions between H_2O and Si-O-Si and between H_2O/O_2 and oxygen-deficient centres (E' defect centre) have been calculated from ab-initio calculations [33]. For the case of interstitial H_2O + Si-O-Si reaction, the formation of silanol groups (Si-OH) has the lowest energy barrier in the range of 0.3 to 0.7 eV. For the case of the interstitial H_2O + E' reaction, the reaction is exothermic (+1.4 eV) with an energy barrier of 1.8 and 1.3 eV if the vacancy is neutral or charged respectively. In

the case of E' + O_2 reaction, there is no energy barrier and the reaction is exothermic with an energy release of about 4.5 eV. Compared to the energy barrier for water diffusion through large rings (~ 0.8 eV), the E' + H_2O is reaction limited whereas E'+O_2 is diffusion limited. These low and no-energy-barrier exothermic reactions with defects in the irradiated glass should provide favorable transport pathways which would be limited or absent in the non-irradiated glass. It is therefore plausible that the overall outcome of irradiation-induced point defects would be to increase the reactivity of the glass and the rate of alteration at least when the water transport within the glass is not significantly affected by the precipitated phases and the alteration layer.

It is worth highlighting that detailed studies to identify various irradiation-induced point defects in the ISG glass need to be undertaken. A very good overview of various defect types in amorphous SiO_2 is presented in L. Skuja *et al.*[41]. Techniques such as UV-Visible spectroscopy, EPR and photoluminescence could be indispensable tools in this regard. Such studies could then be complemented by ab-initio simulations of the reactions of water with various defect types to better understand how irradiation-induced defects would affect the chemical reactivity of the ISG glass.

5.1.4 Changes in the ring size-distribution

First-principles calculations on the diffusion of O_2 and H_2O through amorphous SiO_2 [33] have shown that energy barrier for water diffusion through 4, 5, 6 and 7 member rings is about 2, 1.8, 0.85 and 0.8 eV respectively and that the water diffusion primarily takes place through six-member and larger rings with small energy barriers (~ 0.8 eV). Based on an earlier work on the MD simulation of radiation damage in simple borosilicate glasses [31], the distribution of rings in a sodium borosilicate glass (with same R ($[Na_2O]/[B_2O_3]$) and K ($[SiO_2]/[B_2O_3]$) as the ISG glass) before and after radiation damage (Figure S3 in the SI) shows that there is an increase in the fraction of the 10-member and larger rings and 3-member rings after radiation damage. Furthermore, our earlier MD simulations of radiation damage in amorphous SiO_2 have shown an increase in the fraction of large voids [42]. Therefore, the formation of larger rings and voids due to radiation damage, as predicted by MD simulations, would help increase the diffusion of water through the glass network and consequently accelerate the rate of leaching. Furthermore, energy barriers for the fracture [43] and hydrolysis [44] of Si-O-Si bonds in 3 to 5-member rings have been calculated based on molecular orbital calculations using unrestricted Hartree Fock theory. The fracture energy barriers range from about 77 to 103 kcal/mol whereas energy barrier for the hydrolysis of 3, 4 and 5-member rings have been estimated to be 7, 29 and 39 kcal/mol respectively (fracture in presence of water). These estimates show that 3-member rings are easiest to hydrolyse and going by the predictions of the MD simulations — which show an increase in their proportion — radiation-damaged network should provide pathways for easier hydrolysis. This point was also noticed by Bunker [15]. Thus, in a radiation-damaged network, larger rings can offer pathways for faster water diffusion and smaller rings can provide pathways for easier hydrolysis leading to an acceleration in the leaching.

In summary, irradiation-induced modifications that can render the ISG glass structure prone to water attack and make it vulnerable to leaching. To precisely identify the contributions of each of these mechanisms is beyond the scope of this article but the indication is that the majority of the contributions listed above can accelerate the rate of leaching, by affecting one or several fundamental leach mechanisms. We are now going to discuss the isotopic exchanges taking place in the alteration layer and the potential impact of irradiation on the alteration layer microstructure.

5.2 Formation of alteration layer, reactive interface and rate-limiting factors

When comparing the microstructure of alteration layers in the irradiated and non-irradiated ISG glass, essentially, no differences were observed after 13 days of leaching whereas the microstructures after 58 days were strikingly different. For the irradiated ISG glass, the study revealed the development of a porous alteration layer with time. Judging by the results of the 13 and 58 days of leaching, one could infer that maturation of the alteration layer and the formation of porosity took at least 13 days and less than 45 days in the irradiated glass. The fact that no porosity was observed in the non-irradiated glass does not mean that porosity is specifically associated with radiation damage. Studies using spectroscopic ellipsometry on a pristine ISG glass leached for 1625 days at pH 7 and 90° C have also shown the formation of porosity. In addition, we also analyzed a non-irradiated ISG specimen leached for about 1 year at pH 7 and 90° C with the TEM which showed a similar porous layer (TEM work unpublished, the rest has been published in earlier work [7]). Therefore, the current results highlight that the maturation of the alteration layer into a porous gel takes place faster in the irradiated glass. Nonetheless, more detailed microstructural characterisation would be needed to pin down the time scales needed for gel maturation, especially, for the non-irradiated glass where it seems to be a slow process. The fact that the gel maturation is faster in the irradiated glass is in agreement with the potential effects of radiation damage discussed in section 5.1 (i.e. faster water diffusion, faster hydrolysis and, faster condensation reactions and structural relaxation).

Despite the lack of porosity after 13 days of leaching (as revealed by the TEM), the ion irradiated glass had an alteration thickness about 6 times the alteration thickness of the non-irradiated glass (see Figure 2(f)). This indicates it is rather the glass network damage (as discussed in section 5.1) that accelerated the rate of leaching and not necessarily the porosity. From this perspective, the development of porosity only seems to be an aftermath of the condensation reactions and structural relaxations with potentially no major contribution in the initial hydrolysis of the glass network. However, the $^{18}O/^{16}O$ ratio in the "flat front" after short contact duration of 3 minutes and 3 hours showed an increase by a factor of 2 and 36 % respectively in the irradiated glass compared to the non-irradiated one. This indicates that the nature and behaviour of alteration layers, formed as a result of the leaching, towards water diffusion at room temperature was moderately affected by prior irradiation. The initial increase is potentially a result of the porosity as revealed by the TEM leading to an initial enhancement in water ingress. The current results are insufficient to address this point in detail because the transport can be affected by the interconnection of the pores. Some earlier publications have proposed/hypothesized existence of open channels and closed pores that can facilitate water transport [7]. In light of this hypothesis, one could propose that some open channels connecting the ISG glass alteration layer to the outside solution may have contributed to the initial increase of δ in the "flat front" of the irradiated sample. However, further studies focused on evaluating the 3D size distribution of porosity, their inter-connectivity and links to the outside solution are needed in the future. On the other, the long duration immersion experiment showed only about 36 % higher value of δ (in the "flat front") for the irradiated specimen. This difference being within or marginally above the uncertainty values suggests that the interaction between water and alteration layer was only moderately affected by prior irradiation (if any at all). This has also been observed on glasses irradiated by electrons, where the gel formed from the irradiated glass was similar to the one formed from the non-irradiated glass [18]. Therefore, once formed, the gel part of the alteration layers essentially lose any history of radiation damage of the parent glass and behave almost similarly in both the cases with respect to water exchange. This is not unusual because the impact of radiation damage is essentially to modify the rates of reactions at various stages (at the reactive interface) but once a complete structural relaxation has taken place, the final gel structure will be free of any history of the parent glass and the associated reaction rates.

In stark contrast to the $^{18}O/^{16}O$ ratio in the "flat front" where ^{18}O enrichment tended towards saturation over time, the ^{18}O enrichment at the reactive interface (i.e. SAL) did not show any such tendency in the irradiated specimen. After 82 days, the value of δ for the irradiated specimen was

about twice the value for the non-irradiated one. A higher value of δ for the irradiated specimen is not surprising because radiation-damaged glass network can have a higher reactivity than the pristine one (as discussed earlier). Since the alteration layer after 82 days (~ 600 nm) is less than the radiation damage depth (damage depth ~1000 nm), it is plausible to propose that the rates of room temperature hydrolysis and other reactions in the interface region are higher in the irradiated specimen compared to the non-irradiated specimen. These higher reaction rates can lead to more exchanges/incorporation of ^{18}O at the reactive interface via hydrolysis and condensation reactions , as it is possible that some defects generated by the previous irradiation still exist and contribute to the higher reaction rate in this region. This is not necessarily true for the "flat front" region which essentially consists of a less reactive silica-rich gel already formed at 90°C with very little or no residual radiation damage. This hypothesis can be easily proved if a significantly longer leaching experiment (followed by $H_2{}^{18}O$ immersion) was conducted such that the alteration layer on the irradiated specimen extended far beyond the radiation-damaged depth. In this case, the reactive interface will have moved to the pristine region and the value of δ can be expected to drop back to the one seen in the pristine specimen. In any case, the higher reactivity of the reactive interface makes one wonder whether the rate of reaction at the interface is limited by the transport through the alteration layer or by the reaction rates at the reactive interface (or by a combination of both). It is a question of fundamental importance that needs to be addressed to understand the rate-limiting mechanisms and approach to the so-called "residual rate". Therefore, further in-depth research needs to be undertaken on this subject to address questions such as these.

6 Conclusion

Specimens of ISG glass were first irradiated with multi-energy gold ions (0.5 – 3.5 MeV) to simulate the effect of recoil nucleus damage. These irradiated specimens were then subjected to leaching in water for up to 82 days at 90 °C and pH 9 under static conditions. After leaching, focused ion beam milling was used to extract thin TEM lamellae from the irradiated and non-irradiated specimens leached for 13 and 58 days and characterized using TEM and EFTEM. In addition, specimens leached for 82 days were immersed in isotopically tagged water ($H_2{}^{18}O$) at room temperature and analyzed using ToF-SIMS from 3 minutes to 3413 hours of immersion at regular intervals to track the ingress of isotopically tagged water and ^{18}O -^{16}O exchanges as a function of the immersion time.

The EFTEM showed the development of boron depleted alteration layers in both the irradiated and non-irradiated ISG glass, in excellent agreement with the earlier ToF-SIMS results [23]. After 13 days of leaching of the irradiated glass, the TEM images revealed the formation of a non-porous alteration layer of about 237 nm (~ 40 nm in the non-irradiated specimen). However, after 58 days of leaching of the irradiated specimen, an alteration layer of 570 nm (~138 nm in the non-irradiated specimen) that consisted of an outer porous region of about 480 nm (~ 86% of the alteration layer thickness) and an inner non-porous region of about 80 nm was observed. Besides being significantly smaller, the alteration layers in the non-irradiated glasses were non-porous in all the studied cases and the alteration thicknesses evaluated using both TEM and EFTEM were in excellent agreement with the earlier ToF-SIMS results. In addition to showing that the radiation damage accelerated the rate of leaching, the results highlight that radiation damage can also accelerate subsequent maturation of alteration layer into a porous gel-like microstructure. Based on the results thus far, we conclude that the maturation of the alteration layer into a porous structure took at least 13 days and at most 45 days (58 minus 13 days) in the irradiated glass. As no porosity was observed in the non-irradiated glass even after 58 days, it is plausible to assume that the maturation process would take more than 58 days. Additional studies are needed to precisely evaluate the gel maturation times for the irradiated and the non-irradiated ISG glass.

By using ToF-SIMS to track ^{18}O as a function of the specimen depth and immersion time in $H_2{}^{18}O$, the alteration layer could be divided into two regions depending on the degree of ^{18}O enrichment. The

most significant increase in the ^{18}O enrichment was observed at the interface of the altered layer and the non-altered glass (i.e. at the reactive interface) where a sharp spike in ^{18}O signal was observed compared to the rest of the alteration layer. Moreover, the spike in the irradiated glass was about twice the spike in the non-irradiated glass after 3413 hours of immersion. It was concluded that the higher ^{18}O signal at the interface was due to higher reactivity of water at room temperature with the "glassy material" at the reactive interface compared to the boron and alkali depleted silica-rich gel-layer formed after leaching. Furthermore, radiation damage introduced additional reactive defects and structural changes (changes in boron coordination, ring size distribution etc) which could further increase the reactivity of both the glass and the reactive interface layer. This was essentially manifested in the relatively higher ^{18}O spike at the reactive interface in the irradiated glass compared to the non-irradiated glass. In contrast, the ^{18}O enrichment in most of the alteration layer was lower and almost flat (referred as "flat region") from the surface up to almost the reactive interface - where the spike was observed. Furthermore, the differences in ^{18}O enrichment in the "flat region" of the alteration layer on the irradiated and the non-irradiated glass decreased as a function of the immersion time. The irradiated glass initially showed an ^{18}O signal twice the signal on the non-irradiated glass but this eventually dropped to just about differences within the uncertainty value for the irradiated glass after 3413 hours of immersion. It is plausible to propose that the presence of porosity in the irradiated glass may have contributed to the initial increase but in the long-term, the alteration layers behaved similarly reflecting their inherent reactivity. These results highlight that the long-term reactivity of the gel-layer at room temperature does not have a significant dependence on the prior radiation damage to the parent glass. Thus, although the rates of the leaching and gel maturation are affected by radiation damage, the final relaxed gel does not seem to retain a significant history of radiation damage. In essence, the isotope tracing experiments point out the important role the reactive interface plays in the irradiated as well as in the non-irradiated glass and highlight that the chemical reactivity at this interface could be the driving force for glass leaching. From this perspective, more studies focussing on the behaviour of the reactive interface in irradiated and non-irradiated glasses are needed to understand the mechanisms controlling the glass dissolution in the residual alteration rate regime.

7 Supporting information

Supplementary information is available in a "supplementary information" file. The information concern low magnification TEM image of the pre-irradiated ISG glass sample leached for 58 days, showing the partially detached Cr coating (fig S1), and some details of results contained in ref 39 (fig S2) and ref 31 (fig S3) in order to improve the discussion about some specific points.

8 Acknowledgements

The authors are grateful to the Engineering and Physical Sciences Research Council, UK for funding under grants EP/T012811/1, EP/ E017266/1, EP/M011135/1 and EP/M028283/1 and to Orano/EDF, France for funding the PhD thesis of one of the co-authors. The authors are also thankful for the support the IAEA provided through the INWARD coordinated research project (F11022, 2018 – 2022) promoting collaborative research. We would also like to thank Laurent Dupuy, Elodie Chauvet and Yves de Puydt for ToF-SIMS characterizations and Stéphane Gin for fruitful discussions. The authors also thank Amreen Jan for sharing her molecular dynamics data shown in the SI.

9 References

(1) Doremus, R. H. Interdiffusion of hydrogen and alkali ions in a glass surface. *Journal of Non-Crystalline Solids* **1975**, *19*, 137-144.

(2) Rébiscoul, D.; Bruguier, F.; Magnin, V.; Gin, S. Impact of soda-lime borosilicate glass composition on water penetration and water structure at the first time of alteration. *Journal of Non-Crystalline Solids* **2012**, *358*, 2951-2960.

(3) Bouyer, F.; Geneste, G.; Gin, S. Hydrogen-sodium interdiffusion in borosilicate glasses investigated from first principles. *Journal of Non-Crystalline Solids* **2006**, *352*, 3147-3152.

(4) Rébiscoul, D.; Rieutord, F.; Né, F.; Frugier, P.; Cubitt, R.; Gin, S. Water penetration mechanisms in nuclear glasses by X-ray and neutron reflectometry. *Journal of Non-Crystalline Solids* **2007**, *353*, 2221-2230.

(5) Advocat, T.; Crovisier, J. L.; Vernaz, E.; Ehret, G.; Charpentier, H.: Hydrolysis of R7T7 nuclear waste glass in dilute media : mechanisms and rates as a function of pH. In *Scientific Basis for Nuclear Waste Management Xiv*; Abrajano, T. A., Johnson, L. H., Eds.; Materials Research Society: Pittsburgh, 1991; Vol. 212; pp 57-64.

(6) Hellmann, R.; Cotte, S.; Cadel, E.; Malladi, S.; Karlsson, L. S.; Lozano-Perez, S.; Cabie, M.; Seyeux, A. Nanometre-scale evidence for interfacial dissolution-reprecipitation control of silicate glass corrosion. *Nature Materials* **2015**, *14*, 307-311.

(7) Gin, S.; Collin, M.; Jollivet, P.; Fournier, M.; Minet, Y.; Dupuy, L.; Mahadevan, T.; Kerisit, S.; Du, J. Dynamics of self-reorganization explains passivation of silicate glasses. *Nat Commun* **2018**, *9*, 2169.

(8) Valle, N.; Verney-Carron, A.; Sterpenich, J.; Libourel, G.; Deloule, E.; Jollivet, P. Elemental and isotopic (Si-29 and O-18) tracing of glass alteration mechanisms. *Geochim. Cosmochim. Acta* **2010**, *74*, 3412-3431.

(9) Mercado-Depierre, S.; Fournier, M.; Gin, S.; Angeli, F. Influence of zeolite precipitation on borosilicate glass alteration under hyperalkaline conditions. *J. Nucl. Mater.* **2017**, *491*, 67-82.

(10) Gin, S.; Jollivet, P.; Fournier, M.; Angeli, F.; Frugier, P.; Charpentier, T. Origin and consequences of silicate glass passivation by surface layers. *Nature Communications* **2015**, *6*, 8.

(11) Geisler, T.; Janssen, A.; Scheiter, D.; Stephan, T.; Berndt, J.; Putnis, A. Aqueous corrosion of borosilicate glass under acidic conditions: A new corrosion mechanism. *Journal of Non-Crystalline Solids* **2010**, *356*, 1458-1465.

(12) Lenting, C.; Plümper, O.; Kilburn, M.; Guagliardo, P.; Klinkenberg, M.; Geisler, T. Towards a unifying mechanistic model for silicate glass corrosion. *npj Materials Degradation* **2018**, *2*, 28.

(13) Cailleteau, C.; Angeli, F.; Devreux, F.; Gin, S.; Jestin, J.; Jollivet, P.; Spalla, O. Insight into silicate-glass corrosion mechanisms. *Nature Materials* **2008**, *7*, 978-983.

(14) Gin, S.; Jollivet, P.; Rossa, G. B.; Tribet, M.; Mougnaud, S.; Collin, M.; Fournier, M.; Cadel, E.; Cabie, M.; Dupuy, L. Atom-Probe Tomography, TEM and ToF-SIMS study of borosilicate glass alteration rim: A multiscale approach to investigating rate-limiting mechanisms. *Geochim. Cosmochim. Acta* **2017**, *202*, 57-76.

(15) Bunker, B. C. Molecular mechanisms for corrosion of silica and silicate glasses. *Journal of Non-Crystalline Solids* **1994**, *179*, 300-308.

(16) Geisler, T.; Dohmen, L.; Lenting, C.; Fritzsche, M. B. K. Real-time in situ observations of reaction and transport phenomena during silicate glass corrosion by fluid-cell Raman spectroscopy. *Nat Mater* **2019**, *18*, 342-348.

(17) Gin, S.; Jollivet, P.; Tribet, M.; Peuget, S.; Schuller, S. Radionuclides containment in nuclear glasses: an overview. *Radiochim. Acta* **2017**, *105*, 927-959.

(18) Mougnaud, S.; Tribet, M.; Renault, J. P.; Jollivet, P.; Panczer, G.; Charpentier, T.; Jegou, C. Effect of low dose electron beam irradiation on the alteration layer formed during nuclear glass leaching. *J. Nucl. Mater.* **2016**, *482*, 53-62.

(19) Rolland, S.; Tribet, M.; Jegou, C.; Broudic, V.; Magnin, M.; Peuget, S.; Wiss, T.; Janssen, A.; Blondel, A.; Toulhoat, P. Tc-99- and Pu-239-Doped Glass Leaching Experiments: Residual Alteration Rate and Radionuclide Behavior. *Int. J. Appl. Glass Sci.* **2013**, *4*, 295-306.

(20) Rolland, S.; Tribet, M.; Jollivet, P.; Jegou, C.; Broudic, V.; Marques, C.; Ooms, H.; Toulhoat, P. Influence of gamma irradiation effects on the residual alteration rate of the French SON68 nuclear glass. *J. Nucl. Mater.* **2013**, *433*, 382-389.

(21) Peuget, S.; Delaye, J. M.; Jegou, C. Specific outcomes of the research on the radiation stability of the French nuclear glass towards alpha decay accumulation. *J. Nucl. Mater.* **2014**, *444*, 76-91.

(22) Peuget, S.; Tribet, M.; Mougnaud, S.; Miro, S.; Jegou, C. Radiation effects in ISG glass: from structural changes to long term aqueous behavior. *NPJ Materials Degradation* **2018**, *2:23*.

(23) Mougnaud, S.; Tribet, M.; Renault, J. P.; Gin, S.; Peuget, S.; Podor, R.; Jegou, C. Heavy ion radiation ageing impact on long-term glass alteration behavior. *J. Nucl. Mater.* **2018**, *510*, 168-177.

(24) Lonartz, M. I.; Dohmen, L.; Lenting, C.; Trautmann, C.; Lang, M.; Geisler, T. The Effect of Heavy Ion Irradiation on the Forward Dissolution Rate of Borosilicate Glasses Studied in Situ and Real Time by Fluid-Cell Raman Spectroscopy. *Materials* **2019**, *12*, 1480.

(25) Schindelin, J.; Arganda-Carreras, I.; Frise, E.; Kaynig, V.; Longair, M.; Pietzsch, T.; Preibisch, S.; Rueden, C.; Saalfeld, S.; Schmid, B.; Tinevez, J.-Y.; White, D. J.; Hartenstein, V.; Eliceiri, K.; Tomancak, P.; Cardona, A. Fiji: an open-source platform for biological-image analysis. *Nature Methods* **2012**, *9*, 676-682.

(26) Jouzel, J.: Water stable isotopes: atmospheric composition and applications in polar ice core studies. Isotope Geochemistry. In *The treatise on geochemistry* Elsevier ed.; H. D. Holland, K. K. T., Ed., 2011; pp 151-180.

(27) Charpentier, T.; Martel, L.; Mir, A. H.; Somers, J.; Jégou, C.; Peuget, S. Self-healing capacity of nuclear glass observed by NMR spectroscopy. *Scientific Reports* **2016**, *6*, 25499.

(28) Mir, A. H.; Monnet, I.; Toulemonde, M.; Bouffard, S.; Jegou, C.; Peuget, S. Mono and sequential ion irradiation induced damage formation and damage recovery in oxide glasses: Stopping power dependence of the mechanical properties. *J. Nucl. Mater.* **2016**, *469*, 244-250.

(29) Mir, A. H.; Peuget, S.; Toulemonde, M.; Bulot, P.; Jegou, C.; Miro, S.; Bouffard, S. Defect recovery and damage reduction in borosilicate glasses under double ion beam irradiation. *Epl* **2015**, *112*, 36002.

(30) Mendoza, C.; Peuget, S.; Charpentier, T.; Moskura, M.; Caraballo, R.; Bouty, O.; Mir, A. H.; Monnet, I.; Grygiel, C.; Jegou, C. Oxide glass structure evolution under swift heavy ion irradiation. *Nuclear Instruments and Methods in Physics Research Section B: Beam Interactions with Materials and Atoms* **2014**, *325*, 54-65.

(31) Jan, A.; Delaye, J.-M.; Gin, S.; Kerisit, S. Molecular dynamics simulation of ballistic effects in simplified nuclear waste glasses. *Journal of Non-Crystalline Solids* **2019**, *505*, 188-201.

(32) Jan, A.; Delaye, J.-M.; Gin, S.; Kerisit, S. Monte Carlo simulation of the corrosion of irradiated simplified nuclear waste glasses. *Journal of Non-Crystalline Solids* **2019**, *519*, 119449.

(33) Bakos, T.; Rashkeev, S. N.; Pantelides, S. T. Reactions and Diffusion of Water and Oxygen Molecules in Amorphous SiO2. *Physical Review Letters* **2002**, *88*, 055508.

(34) Delaye, J. M.; Ghaleb, D. Molecular dynamics analysis of volume change in a nuclear glass model subjected to a displacement cascade. *Nuclear Instruments and Methods in Physics Research Section B: Beam Interactions with Materials and Atoms* **1999**, *153*, 157-162.

(35) Maugeri, E. A.; Peuget, S.; Staicu, D.; Zappia, A.; Jegou, C.; Wiss, T.; Jantzen, C. Calorimetric Study of Glass Structure Modification Induced by α Decay. *Journal of the American Ceramic Society* **2012**, *95*, 2869-2875.

(36) Du, T.; Li, H.; Sant, G.; Bauchy, M. New insights into the sol–gel condensation of silica by reactive molecular dynamics simulations. *The Journal of Chemical Physics* **2018**, *148*, 234504.

(37) Peuget, S.; Broudic, V.; Jegou, C.; Frugier, P.; Roudil, D.; Deschanels, X.; Rabiller, H.; Noel, P. Y. Effect of alpha radiation on the leaching behaviour of nuclear glass. *J. Nucl. Mater.* **2007**, *362*, 474-479.

(38) Tribet, M.; Rolland, S.; Peuget, S.; Broudic, V.; Magnin, M.; Wiss, T.; Jégou, C. Irradiation Impact on the Leaching Behavior of HLW Glasses. *Procedia Materials Science* **2014**, *7*, 209-215.

(39) Stone-Weiss, N.; Pierce, E. M.; Youngman, R. E.; Gulbiten, O.; Smith, N. J.; Du, J. C.; Goel, A. Understanding the structural drivers governing glass-water interactions in borosilicate based model bioactive glasses. *Acta Biomater.* **2018**, *65*, 436-449.

(40) Angeli, F.; Charpentier, T.; Jollivet, P.; de Ligny, D.; Bergler, M.; Veber, A.; Gin, S.; Li, H. Effect of thermally induced structural disorder on the chemical durability of International Simple Glass. *npj Materials Degradation* **2018**, *2*, 31.

(41) Skuja, L. Optically active oxygen-deficiency-related centers in amorphous silicon dioxide. *Journal of Non-Crystalline Solids* **1998**, *239*, 16-48.

(42) Mir, A. H.; Hinks, J. A.; Delaye, J.-M.; Peuget, S.; Donnelly, S. E. Xenon solubility and formation of supercritical xenon precipitates in glasses under non-equilibrium conditions. *Scientific Reports* **2018**, *8*, 15320.

(43) West, J. K.; Hench, L. L. Silica fracture. *Journal of Materials Science* **1994**, *29*, 3601-3606.

(44) West, J. K.; Hench, L. L. Silica fracture. *Journal of Materials Science* **1995**, *30*, 6281-6287.